Microphase Separation of Segmented Poly(urethane urea) Block Copolymers

J. T. Garrett and J. Runt*

Department of Materials Science and Engineering, The Pennsylvania State University, University Park, Pennsylvania 16802

J. S. Lin

Oak Ridge National Laboratory, Oak Ridge, Tennessee 37831

Received April 4, 2000; Revised Manuscript Received June 21, 2000

ABSTRACT: Two series of well-defined poly(urethane urea) multiblock copolymers were synthesized to investigate the phase-separated morphology of this family of materials. Series I copolymers were synthesized from 2000 g/mol poly(tetramethylene oxide) [PTMO], 4,4′-methylene di(*p*-phenyl isocyanate) [MDI], and ethylenediamine (EDA), with hard segment contents ranging from 14 to 47 wt %. Series II copolymers (all with hard segment concentrations of 22 wt %) were prepared from the same PTMO and MDI and a diamine mixture of EDA and 1,4-diaminocyclohexane. The microdomain morphology was characterized using small-angle X-ray scattering, and the scattering data were analyzed using the approach of Bonart and Müller. The series I and II copolymers were found to have relatively low overall degrees of phase separation [ranging from ∼20% at the lowest hard segment contents to greater than 40%], contrary to the common notion that these copolymers are well phase separated materials. The introduction of the second diamine results in reduced phase separation, presumably as a consequence of disruption of hard segment hydrogen bonding.

I. Introduction

Since the early work of Cooper and Tobolsky,[1] it has been established that segmented polyurethane block copolymers generally microphase separate into high-T_g (sometimes crystalline) "hard" domains and relatively low-T_g "soft" domains, on cooling from the melt or precipitation from solution. The degree to which these copolymers phase separate significantly affects many of the physical properties of these materials.[2−10] Phase separation has been studied using a number of techniques, most notably small-angle X-ray scattering (SAXS).[3,8,11−15]

In the present paper we focus on a subclass of segmented polyurethanes, the poly(urethane urea)s [PUU], in which diamines are used as the chain extenders rather than diols. It has been found that poly(urethane urea) elastomers possess improved mechanical properties compared to traditional polyurethane elastomers[16,17] due, in part, to the stronger hydrogen bonding in the hard domains. The urea groups not only provide additional hydrogen-bonding sites, but interurea hydrogen bonds have a stronger, three-dimensional nature.[5,18,19] Unfortunately, the hydrogen bonding is so strong in some cases that the materials cannot be processed from the melt without degradation. Poly(urethane urea)s have become increasingly popular and are used in a variety of applications,[10] including as the blood-contacting material in total artificial hearts and the left ventricular assist devices.[21,22]

Despite the relative importance of PUUs, there has been limited research directed toward understanding phase separation in these materials and the role of thermal history on the microphase separated structure. In this paper, we present a quantitative SAXS investigation of two series of well-defined poly(urethane urea)s synthesized from 4,4′-methylene di(*p*-phenyl isocyanate) (MDI), poly(tetramethylene oxide), and ethylenediamine (and a diamine mixture).

II. Experimental Section

Materials. Two series of model poly(urethane urea)s were synthesized via a two-step condensation reaction. They were prepared using a 2000 g/mol poly(tetramethylene oxide) (PTMO), end-capped with 4,4′-methylene di(*p*-phenyl isocyanate), and chain extended by ethylenediamine (EDA) or a diamine mixture [EDA and 1,4-diaminocyclohexane (DACH)], in a solution of *N*,*N*-dimethylacetamide (DMAc, 99+%, anhydrous). All of the above were purchased from Aldrich Chemical, Co. MDI was purified by distillation and transferred to a glovebox, which was kept under an inert argon atmosphere. PTMO (3 wt %) was dissolved in DMAc and stirred in a flask while MDI was added to the solution. These two reactants were heated to 80 °C and held there for 2 h. The reaction vessel was cooled to room temperature before the chain extender (diamine) was added. The diamine was diluted in DMAc and dripped into the stirring reaction, facilitating efficient distribution of the diamine throughout the reaction mixture. The reaction was then stirred for approximately 1 h. All copolymers remained in solution during the course of the polymerization reaction. Finally, Santowhite powder (Solutia, Inc.), an antioxidant, was added at 1 wt %.

Only EDA was used as the chain extender in the first group of polymers, referred to in this paper as series I. The series I copolymers are identified by "PUU" and a number denoting the hard segment weight fraction which is calculated by assigning all MDI and EDA units to the hard segment. All polymers in series II have the same hard segment weight fraction (22%), but some EDA was replaced with DACH such that the relative molar ratio of EDA as the chain extender varied from 1 to 0.65. The second diamine was incorporated in an attempt to partially disrupt hydrogen bonding in the hard phase. For the identification of the series II copolymers, the hard segment weight fraction appears first, followed by the percentage of total diamine that is DACH.

* To whom correspondence should be addressed.

10.1021/ma000600i CCC: $19.00
Published on Web 08/08/2000

Table 1. Molecular Weights of Series I and II Copolymers from GPC

	M_n g/mol	M_w g/mol	M_w/M_n
series I			
PUU 14	31 600	50 900	1.6
PUU 17	36 500	81 400	2.2
PUU 22	24 500	47 800	2.0
PUU 30	14 600	33 300	2.3
PUU 37	13 900	37 900	2.7
PUU 43	8300	20 800	2.5
PUU 47	6300	14 200	2.3
series II			
PUU 22−0	24 500	47 800	2.0
PUU 22−5	20 600	39 800	1.9
PUU 22−15	20 400	46 000	2.3
PUU 22−25	28 000	57 600	2.1
PUU 22−35	25 100	76 300	3.0

Gel Permeation Chromatography. All polymers were initially characterized using gel permeation chromatography (GPC). Dimethylformamide (DMF) containing 0.05 M lithium bromide was used as the mobile phase. The experiments were conducted using a Waters model 510 pump and a model 410 refractive index detector. Samples were run at 80 °C through two PLgel 5 μm Mixed-C columns (Polymer Laboratories). Data analysis was performed using Waters Millennium Chromatography Manager software. Calibration was performed using narrow molecular weight distribution (M_w/M_n < 1.1) poly(ethylene oxide) standards (Polymer Standards Service−USA), ranging from 10 000 to 963 000 g/mol.

The results of the GPC experiments are summarized in Table 1. A polydispersity index around 2 is typical for condensation polymerizations. It is clear from Table 1 that the apparent molecular weight decreases with increasing hard segment content. This is expected and is simply a function of the reactant ratios.[13]

Sample Preparation. Samples for the small-angle X-ray scattering experiments were prepared as follows. The as-polymerized solutions (~3 wt %) were poured into shallow circular disks and placed under vacuum at room temperature for 24 h. The oven temperature was then raised to 70 °C and maintained at this temperature for an additional 24 h. Films were on the order of 100 μm thick. Films of higher hard segment copolymers were generally thinner to avoid skinning during casting. The films were cut into 1 cm × 1 cm squares and stacked to a thickness of approximately 1 mm. The films have a high affinity for each other, so the squares adhered well. Samples of all series I and II copolymers were prepared using this approach.

Small-Angle X-ray Scattering. SAXS experiments were conducted on the Oak Ridge National Laboratory 10 m pinhole collimated SAXS camera using Cu Kα radiation (wavelength, λ = 0.154 nm) and a 20 cm × 20 cm positional sensitive proportional detector. Scattered intensities were stored in a 64 × 64 array. Instrument background corrections and detector efficiency were determined with an ^{55}Fe radioactive sample. Each sample was run at two different sample-to-detector distances, 1.119 and 5.119 m, to give a q range of q = 0.0614−4.595 nm^{-1}. Here $q = (4\pi/\lambda)\sin(\theta/2)$ where θ is the scattering angle. The two-dimensional data were azimuthally averaged to give a one-dimensional profile. The relative scattering intensities were converted to absolute intensities via precalibrated secondary standards: a high-density polyethylene for the low-q data and a vitreous carbon for the high-q data.

The 1 and 5 m data were suitably appended to yield one data set for each sample. These data were then corrected for background noise and thermal density fluctuations. Since high-q data are available, a q-dependent background correction was performed via the method of Ruland.[24] This involves fitting the high-q data (in the Porod region) to an exponential function by adjusting constants a and b:

$$I_b(q) = a e^{bq^2} \quad (1)$$

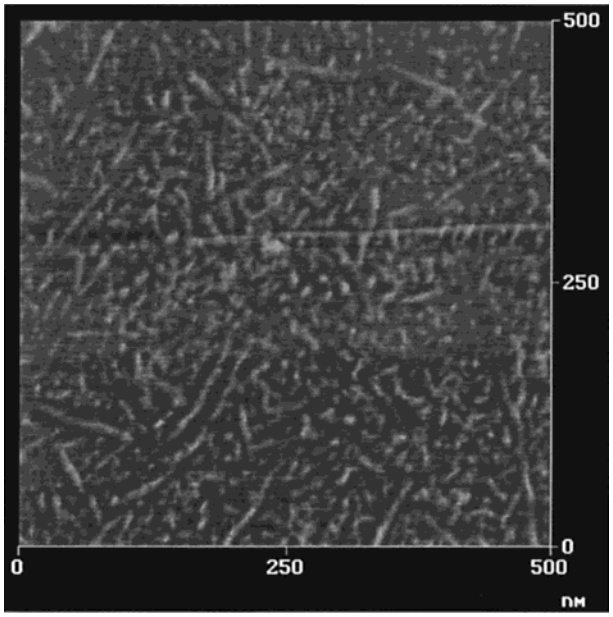

Figure 1. AFM tapping mode phase image of the as-cast surface of PUU 37. Image was obtained with a Digital Instruments Multimode AFM with silicon probe in air; r_{sp} (set point amplitude/free amplitude of oscillation) = 0.95. Image is 500 × 500 nm region.

The background scatter [$I_b(q)$] is calculated over all q and then subtracted from the raw intensities.

III. Results and Discussion

Particularly at higher hard segment contents, the morphology of segmented polyurethane and poly(urethane urea) block copolymers has sometimes been treated as a stacked lamellar structure and the one-dimensional correlation function used to analyze the scattering data.[25−28] It was not clear a priori that such a model was appropriate for the series I and II PUU copolymers, particularly since all hard segment contents are <50 wt %. To shed some light on the hard domain organization, atomic force microscopy (AFM) experiments were conducted in a separate study on all series I and II copolymers.[29] AFM tapping mode phase images show that the hard phases are not stacks of lamellae but can best be described as randomly oriented cylinders with additional spherical domains. This is illustrated in the AFM image of the as cast "surface" of PUU 37 in Figure 1. The hard domains appear as the bright regions and have lateral dimensions on the order of 5−10 nm. A similar morphology is seen for both free surfaces and in microtomed cross sections of solution cast films and is observed for all series I and II copolymers.[29] Consequently, we utilized the general approach of Bonart and Müller[2,3] for analysis of the PUU copolymer scattering data. For a more thorough description of this method, see refs 2 and 14.

A. Analysis. The experimental SAXS curves for the PUU copolymers are presented in Figures 2 and 3. Both the peak positions and total scattering intensities provide important information about the microphase separated structure. The peak position is related to the interdomain spacing, d, by

$$d = \frac{2\pi}{q_{max}} \quad (2)$$

Table 2. Electron Density Variances and Domain Parameters for PUU Copolymers

	$\overline{\Delta\eta_c^2} \times 10^3$ [a]	$\overline{\Delta\eta^{2\prime}} \times 10^3$	$\overline{\Delta\eta^{2\prime\prime}} \times 10^3$	interdomain spacing (nm)	boundary size	
					σ (nm)	E (nm)
series I						
PUU 14	1.09	0.22	0.22	30	0.1	0.2
PUU 17	2.55	0.68	1.03	13.8	0.6	2.0
PUU 22	4.18	1.72	2.33	13.4	0.5	1.7
PUU 30	6.03	1.80	2.27	12.7	0.5	1.7
PUU 37	7.08	2.16	2.42	15.5	0.4	1.3
PUU 43	7.73	1.93	2.28	14.4	0.4	1.6
PUU 47	8.12	2.16	2.60	14.4	0.5	1.6
series II						
PUU 22−0	4.18	1.72	2.33	13.4	0.5	1.7
PUU 22−5	4.19	1.02	1.29	12.3	0.3	1.1
PUU 22−15	4.16	1.06	1.49	11.7	0.6	2.2
PUU 22−25	4.13	1.02	1.29	12.5	0.5	1.7
PUU 22−35	4.09	0.85	1.05	13.6	0.4	1.5
annealing of PUU 43						
70 °C (24 h)	7.73	1.93	2.28	14.4	0.5	1.5
100 °C (5 h)	7.73	2.15	2.77	13.6	0.6	2.0
150 °C (5 h)	7.73	2.48	2.60	14.1	0.3	0.9

[a] Electron variances are given in units of (mol e/cm^3)^2.

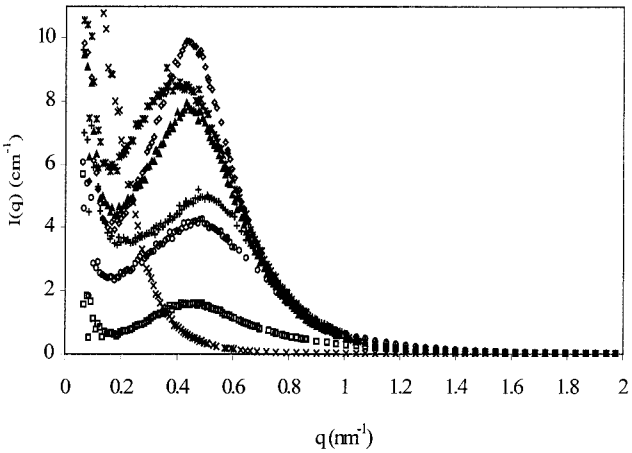

Figure 2. Background corrected SAXS intensities as a function of scattering vector for PUU series I copolymers: ×, PUU 14; □, PUU 17; ○, PUU 22; +, PUU 30; *, PUU 37; ▲, PUU 43; ◇, PUU 47.

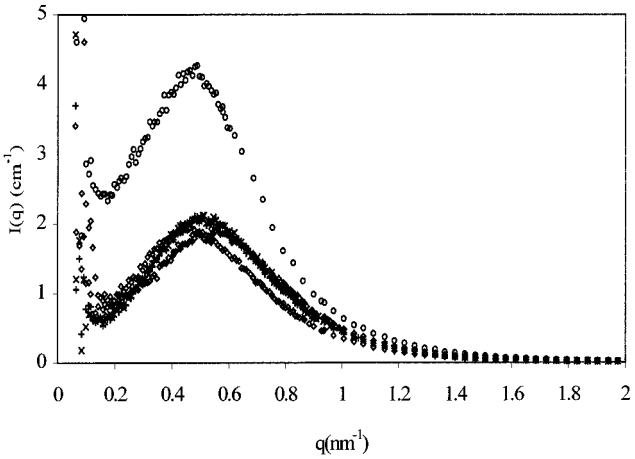

Figure 3. Background corrected SAXS intensities as a function of scattering vector for PUU series II copolymers: ○, PUU 22; ×, PUU 22−5; ◇, PUU 22−15; +, PUU 22−25; □, PUU 22−35.

This spacing represents a three-dimensional average over the sampled volume. For a stacked lamellar morphology, the one-dimensional spacing is generally obtained by defining q_{max} as the q value at maximum intensity of the $I(q)q^2$ vs q plot. Otherwise, as is the case here, q_{max} is the q value at maximum intensity of the $I(q)$ vs q plot.[18] Interdomain spacings for series I and II copolymers are provided in Table 2.

Analysis of the scattering data involves the comparison of a theoretical electron density variance to two experimentally determined variances.[2,14] The theoretical variance is calculated assuming complete phase separation of the hard and soft segments and is defined as

$$\overline{\Delta\eta_c^2} = \phi_{hs}\phi_{ss}(\eta_{hs} - \eta_{ss})^2 \qquad (3)$$

where ϕ_{hs} and ϕ_{ss} are the volume fractions and η_{hs} and η_{ss} are the electron densities of the hard and soft segments, respectively.

The calculation of the theoretical electron density can significantly influence the values determined in this analysis, and it is here that we deviate somewhat from the original approach. Following Bonart and Müller,[2,3] the hard segments would be defined as consisting of *all* MDI and diamine units in the reaction. This would be the case if all PTMO units were double end-capped with MDI units, but MDI groups can react with two PTMO diols, creating what we will subsequently refer to as "lone" MDI units. These lone MDIs introduce no urea groups and are at least 100 bonds away from another MDI unit in the chain. Consequently, these species would not be expected to be associated with the hard domains but be located in the soft phase. The main thrust of the following is to "correct" the theoretical, completely phase separated variance for the presence of lone MDIs in the soft phase.

By following the procedure of Peebles for a two-step condensation polymerization,[31] the distributions of hard segment sequence lengths, from lone MDIs to hard segments containing 21 MDI units and 20 EDA units, were calculated for the series I copolymers. This spread of possibilities accounts for all of the species in all but the three highest hard segment content copolymers. For PUU 37, PUU 43, and PUU 47 it accounts for 99.9%, 99.5%, and 98.5% of the species, respectively. All series II mixed diamine copolymers have the same hard segment length distribution as PUU 22 since the distribution depends only on the concentration and relative reactivity of the diisocyanate and is therefore independent of the chain extender identity.[31]

With these probabilities in hand, the theoretical electron density contribution of the lone MDI units was "removed" from the hard segments and "added" to that of the soft segments. This results in a decrease in the theoretical (completely phase separated) electron density variance, $\overline{\Delta\eta_c^2}$ (relative to the value calculated without considering lone MDIs in the soft phase). These lower values of $\overline{\Delta\eta_c^2}$ are closer to the experimental variances, particularly at lower hard segment concentrations.

Phase densities required to calculate values for $\overline{\Delta\eta_c^2}$ were determined using a group contribution approach,[32] assuming that the soft phase is composed of PTMO and lone MDIs and the hard phase is composed of the remaining MDIs and the diamines. The density of a pure MDI−EDA−MDI hard phase was calculated to be 1.424 g/cm^3, but to our knowledge there have been no reported experimental values with which to compare our result. However, MDI−butanediol (BDO) hard segments are common in the literature, and several groups have estimated the density of a pure MDI−BDO hard phase.[14,33−35] Using the group contribution method, we calculated the density of a pure MDI−BDO hard domain to be 1.382 g/cm^3, which compares well to that determined by Leung and Koberstein (1.354 g/cm^3).[14] We calculated the pure PTMO soft phase density to be 1.009 g/cm^3, and this also compares well with literature values.[3]

Experimental variances are determined from the scattering data and are calculated using the Porod invariant,[36] Q, defined as

$$Q = \int_0^\infty I(q)q^2\,\mathrm{d}q \tag{4}$$

The experimental variances are related to the invariant by a constant, c:

$$\overline{\Delta\eta_c^2} = cQ = c\int_0^\infty I(q)q^2\,\mathrm{d}q \tag{5}$$

where

$$c = \frac{1}{2\pi^2 i_e N_A^2} = 1.76 \times 10^{-24}\ \mathrm{mol^2/cm^2} \tag{6}$$

and i_e is Thompson's constant for the scattering from one electron (7.94×10^{-26} cm^2). N_A is Avogadro's number. Note that only a constant with these units will yield a variance with the appropriate units of (mol e/cm^3)^2.

With the appropriate constant, two variances can be calculated from the experimental data. These are illustrated schematically in Figure 4. The experimental variances are represented in parts a and b, while part c is the case of complete phase separation. Black pixels represent the hard segments, and white pixels represent the soft segments (ignoring lone MDIs for the purposes of illustration). Mixing of unlike segments (pixels) changes the black region to a dark gray and the white region to a light gray.

The first variance is calculated from the background corrected intensities but leaves the influence of diffuse phase boundaries, as seen by the gray scale gradient at the interfaces in Figure 4a. It also includes intermixed segments and is represented as

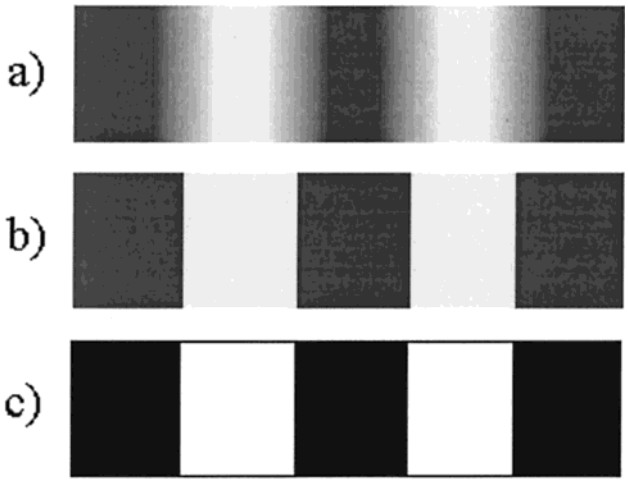

Figure 4. Schematic illustration of electron density differences. Hard segments are black, and soft segments are white. (a) Including contributions from diffuse boundaries and mixing within the domains. (b) Diffuse boundaries removed. (c) Ideal electron density difference (no mixing between the components). Size of the blurred region in (a) is for illustration only and does not represent the relative dimensions of the phase boundaries in the PUU copolymers.

$$\overline{\Delta\eta^{2\prime}} = c\int_0^\infty [I(q) - I_b(q)]q^2\,\mathrm{d}q \tag{7}$$

The second variance (eq 8) removes contributions from diffuse boundaries, which leaves only gray regions (illustrating intermixing), as seen in Figure 4b.

$$\overline{\Delta\eta^{2\prime\prime}} = c\int_0^\infty \frac{[I(q) - I_b(q)]q^2}{H(q)^2}\,\mathrm{d}q \tag{8}$$

This requires the calculation of $H(q)$, which models the size and shape of the interfacial boundary.[37] The shape of the interface can be fit using a linear-gradient model or a sigmoidal-gradient model. The sigmoidal shape seems more likely to occur naturally and is supported by the thermodynamic arguments of Koberstein et al.[37] The characteristic value of the sigmoidal-gradient model, σ, is the standard deviation of the Gaussian function used in the model and was determined from

$$\ln[I(q)q^4] = \ln K_p - \sigma^2 q^2 \tag{9}$$

i.e., from the slope of a $\ln[I(q)q^4]$ vs q^2 plot.

In the linear model, E is defined as the distance from phase A to phase B. The characteristic width parameters from the two models are related by $E^2 = 12\sigma^2$. Even though the sigmoidal model is used in our calculations, the dimension of the linear model is easier to visualize, and both values are reported in Table 2.

By comparing the theoretical variance to the variances defined by eqs 7 and 8, it is possible to gain insight into the overall degree of microphase separation, a measure of boundary diffuseness, and a measure of mixing in the microphases.[2,14]

The ratio of the background corrected experimental variance to the variance calculated assuming complete phase separation

$$\overline{\Delta\eta^{2\prime}}/\overline{\Delta\eta_c^2} \tag{10}$$

Table 3. Electron Density Variance Ratios for PUU Copolymers

	deg of microphase separation $\overline{\Delta\eta^{2\prime}}/\overline{\Delta\eta_c^2}$	boundary diffuseness $\overline{\Delta\eta^{2\prime\prime}}/\overline{\Delta\eta^{2\prime}} - 1$	intermixing within microphases $\overline{\Delta\eta_c^2}/\overline{\Delta\eta^{2\prime\prime}} - 1$	phase separation (%)	boundary effect (%)	intermixing effect (%)
series I						
PUU 14	0.20	0.01	4.0	20	0	80
PUU 17	0.27	0.51	1.5	27	14	59
PUU 22	0.41	0.35	0.8	41	15	44
PUU 30	0.30	0.26	1.7	30	8	62
PUU 37	0.31	0.12	1.9	31	4	65
PUU 43	0.25	0.18	2.4	25	5	70
PUU 47	0.27	0.20	2.1	27	5	68
series II						
PUU 22−0	0.41	0.35	0.8	41	15	44
PUU 22−5	0.24	0.26	2.2	24	6	69
PUU 22−15	0.25	0.41	1.8	25	10	64
PUU 22−25	0.25	0.27	2.2	25	7	69
PUU 22−35	0.21	0.23	2.9	21	5	74
annealing of PUU 43						
70 °C (24 h)	0.25	0.18	2.4	25	5	70
100 °C (5 h)	0.28	0.29	1.8	28	8	64
150 °C (5 h)	0.32	0.05	2.0	32	2	66

provides a measure of overall phase separation. Note that "overall phase separation", as defined here, is influenced by both diffuse phase boundaries and segment intermixing. This ratio returns a value between 0 and 1, with unity indicating complete phase separation. The ratio of $\overline{\Delta\eta_c^2}$ to the experimental value that has had the influence of the interfaces removed

$$(\overline{\Delta\eta_c^2}/\overline{\Delta\eta^{2\prime\prime}}) - 1 \qquad (11)$$

provides a measure of the influence of intermixed segments on overall phase separation. (A value of 0 in eq 11 indicates no mixing between the phases.) Note that this value does not provide insight into the relative amount of hard segments in the soft phase and soft segments in the hard phase without additional information. Finally, the ratio of the two experimental variances

$$(\overline{\Delta\eta^{2\prime\prime}}/\overline{\Delta\eta^{2\prime}}) - 1 \qquad (12)$$

provides a measure of boundary diffuseness. The various ratios defined in eqs 10−12 are summarized in Table 3 for the series I and II copolymers. Overall phase separation and boundary diffuseness values have an uncertainty of approximately 3% of their value, and the intermixing has an uncertainty on the order of 10%.

In addition to the traditional representation, the parameters defined by eqs 10−12 are also provided in Table 3 in a somewhat different fashion. To facilitate an understanding of the latter, the results for PUU 22 will be described. The ratio $\overline{\Delta\eta^{2\prime}}/\overline{\Delta\eta_c^2}$ is 0.41; i.e., the sample is 41% phase separated. Compensating for the influence of diffuse boundaries (that is, for an ideally sharp interface), PUU 22 would be considered 56% phase separated. The difference, 15%, is the relative contribution from the diffuse interface. The remainder of the deviation from $\overline{\Delta\eta_c^2}$, 44%, can be attributed to mixing within the microphases.

B. Discussion. The results in Table 3 clearly indicate a significant degree of phase mixing in the series I and II copolymers, contrary to the common notion that PUUs are well phase separated materials. Longer hard segments are less likely to be soluble in the soft phase, and a greater degree of phase separation is therefore expected for copolymers with higher hard segment contents. This is in fact the general trend observed in the work of Koberstein et al. on compression molded segmented polyurethane block copolymers.[8] For polyurethane hard segment (MDI−butanediol) contents ranging from 30 to 70 wt %, a significant increase in overall phase separation was reported ($\overline{\Delta\eta^{2\prime}}/\overline{\Delta\eta_c^2}$ increases from 0.22 to 0.34). This supports the authors' idea of a critical hard segment sequence length, above which hard segments reside in hard domains, and below which they are dissolved in the soft phase. As hard segment content increases, a greater portion of the sequences is longer than the critical length, increasing the degree of phase separation. However, for an 80 wt % polyurethane copolymer, Koberstein et al. observed a reduction in phase separation and proposed that this was a consequence of constraints in packing long hard segment sequences.

For our PUU 14, the average block length distribution is relatively short, and two-thirds of the MDIs are calculated to be lone MDIs. There is relatively extensive intermixing and a comparatively low degree of phase separation. In fact, the interdomain spacing is largest for this material, indicating the presence of relatively few well-defined domains.

As expected, the degree of phase separation increases significantly upon increasing hard segment content to 17, then 22 wt %, and intermixing is reduced. This lends credence to the idea of a critical hard segment sequence length. Note that in Table 2 there is no systematic change in the interfacial boundary thickness in series I (or series II), with all values in the range of 1−2 nm. Although the size of the interfacial regions are about the same, their contribution to phase separation is larger at lower hard segment concentrations in the series I copolymers (with the exception of the relatively well mixed PUU 14).

For higher hard segment content copolymers, overall phase separation is similar but less than in PUU 22. In addition, intermixing increases for PUU 30, staying approximately constant for higher hard segment content copolymers. This behavior is contrary to expectations, and although the copolymers were effectively annealed for 24 h at 70 °C, it is possible that this behavior arises from the nonequilibrium condition of the higher hard segment content copolymers. These copolymers are less soluble in the DMAc and precipitate earlier in the

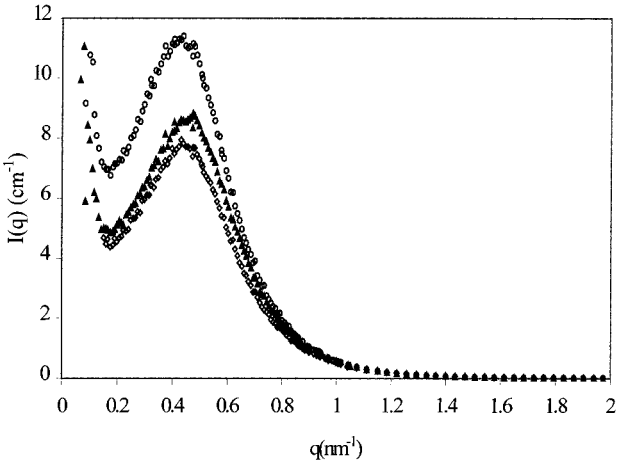

Figure 5. Background corrected SAXS intensities as a function of scattering vector for annealed samples of PUU 43: ◇, 70 °C (24 h); ▲, 100 °C (5 h); ○, 150 °C (5 h).

casting process, likely trapping a nonequilibrium microphase separated morphology.

To investigate this possibility, we conducted further annealing experiments on PUU 43. This copolymer was annealed for 5 h under vacuum at 100 and 150 °C. (Polyurethanes do not undergo degradation or transurethanification at these temperatures.[38]) After annealing, the samples were returned to room temperature and allowed to equilibrate for several days before being analyzed. The scattering curves of the two annealed samples, along with the corresponding specimen dried at 70 °C, are seen in Figure 5. The ratios of the electron density variances (define by eqs 10−12) of these samples are summarized in the bottom portion of Table 3. Both annealing temperatures are above the endothermic transition observed near 60 °C in DSC experiments of the series I and II copolymers. A transition in this temperature range has been assigned to the disruption of short-range order in polyurethanes,[39,40] but its origin has not been explored in PUUs. The annealing temperatures are below a broad transition near 200 °C, which has been characterized as arising from the disruption of long-range order in polyurethanes and as a hard domain T_g in PUUs.[4,28,41]

As seen in Table 3, the degree of phase separation does indeed increase with increasing annealing temperature through a combination of consolidation of the diffuse boundary and reduction in microdomain intermixing. Increasing the annealing temperature from 70 to 100 °C may result in a small increase in boundary size (see Table 2), but mixing in the microphases (see Table 3) is reduced sufficiently to increase overall phase separation. Increasing the annealing temperature further (to 150 °C) results in little change in intermixing, but a significant reduction in the influence of interfacial boundaries leads to an increase in overall phase separation. Although the degree of phase separation for PUU 43 annealed at 150 °C is still below that of PUU 22, we anticipate that it would continue to increase upon annealing for longer times and/or higher temperatures. Such experiments are underway at the present time.

We now turn to the series II copolymers in which a diamine mixture (EDA and DACH) was used in the polymerizations. The most significant difference in the series II copolymers is the drop in phase separation and increase in mixing within the microdomains upon adding DACH, even for as little as 5% of the total diamine content (see Table 3). The DACH disrupts hard segment hydrogen bonding and reduces the driving force for hard segment segregation. PUU 22−5, 22−15, and 22−25 exhibit similar degrees of intermixing, while PUU 22−35 has the highest extent of mixing within the domains and lowest phase separation of the 22 wt % hard segment copolymers.

IV. Conclusions

Two series of poly(urethane urea) multiblock copolymers were synthesized to facilitate an investigation of their microdomain morphology via small-angle X-ray scattering. As expected, overall phase separation increased with increasing hard segment content at lower hard segment concentrations. Average hard segment lengths are longer as hard segment content increases, and the longer segments are less likely to be soluble in the soft phase. This leads to an increase in overall phase separation and a decrease in mixing in the domains. However, above 22 wt % hard segment, the copolymers exhibit a drop in overall phase separation. This is likely due to higher hard segment content copolymers being trapped in a nonequilibrium condition. Annealing experiments conducted on PUU 43 confirmed this. More extensive annealing studies are currently underway.

The addition of as little as 5% of a second diamine, DACH, resulted in a significant reduction in overall phase separation. The copolymer containing the highest DACH concentration, PUU 22−35, had the lowest degree of phase separation of all series II copolymers. The presence of DACH in the hard segment hinders hydrogen bond formation and reduces the driving force for phase separation.

Acknowledgment. We extend our appreciation to Dr. Chris Siedlecki at the Penn State Hershey Medical Center for his invaluable support with the AFM experiments. This research was also supported in part by the Division of Materials Science, U.S. Department of Energy, under Contract DE-AC05-00OR22725 with the Oak Ridge National Laboratory, managed by UT-Battelle, LLC.

References and Notes

(1) Cooper, S. L.; Tobolsky, A. V. *J. Appl. Polym. Sci.* **1966**, *10*, 1837.
(2) Bonart, R.; Müller, E. H. *J. Macromol. Sci., Phys.* **1974**, *B10*, 177.
(3) Bonart, R.; Müller, E. H. *J. Macromol. Sci., Phys.* **1974**, *B10*, 345.
(4) Sung, C. S. P.; Hu, C. B.; Wu, C. S. *Macromolecules* **1980**, *13*, 111.
(5) Sung, C. S. P.; Smith, T. W.; Sung, N. H. *Macromolecules* **1980**, *13*, 117.
(6) Abouzahr, S.; Wilkes, G. L.; Ophir, Z. *Polymer* **1982**, *23*, 1077.
(7) Van Bogart, J. W. C.; Gibson, P. E.; Cooper, S. L. *J. Polym. Sci., Polym. Phys. Ed.* **1983**, *21*, 65.
(8) Christenson, C. P.; Harthcock, M. A.; Meadows, M. D.; Spell, H. L.; Howard, W. L.; Creswick, M. W.; Guerra, R. E.; Turner, R. B. *J. Polym. Sci., Polym. Phys. Ed.* **1986**, *24*, 1401.
(9) Koberstein, J. T.; Galambos, A. F.; Leung, L. M. *Macromolecules* **1992**, *25*, 6195.
(10) Monteiro, E. E. C.; Fonseca, J. L. C. *J. Appl. Polym. Sci.* **1997**, *65*, 2227.
(11) Koberstein, J.T.; Leung, L. M. *Macromolecules* **1992**, *23*, 6205.
(12) Chu, B.; Gao, T.; Li, Y.; Wang, J.; Desper, C. R.; Byrne, C. A. *Macromolecules* **1992**, *25*, 5724.
(13) Tyagi, D.; McGrath, J. E.; Wilkes, G. L. *Polym. Eng. Sci.* **1986**, *26*, 1371.
(14) Leung, L. M.; Koberstein, J. T. *J. Polym. Sci., Polym. Phys. Ed.* **1985**, *23*, 1883.

(15) Koberstein, J.; Stein, R. *J. Polym. Sci., Polym. Phys. Ed.* **1983**, *21*, 1439.
(16) Takahara, A.; Tashita, J.; Kajiyama, T.; Takayanagi, M. *J. Biomed. Mater. Res.* **1985**, *19*, 13.
(17) Hayashi, K.; Takano, H.; Matsuda, T.; Umeza, M. *J. Biomed. Mater. Res.* **1985**, *19*, 179.
(18) Coleman, M. M.; Sobkowiak, M.; Pehlert, G. J.; Painter, P. C. *Macromol. Chem. Phys.* **1997**, *198*, 117.
(19) Teo, L.; Chen, C.; Kuo, J. *Macromolecules* **1997**, *30*, 1793.
(20) Lamba, N. M. K.; Woodhouse, K. A.; Cooper, S. L. *Polyurethanes in Biomedical Applications*; CRC Press: Boca Raton, FL, 1998.
(21) Wu, L.; Weisberg, D.; Runt, J.; Felder, G.; Snyder, A. J.; Rosenberg, G. *J. Biomed. Mater. Res.* **1999**, *44*, 371.
(22) Liu, Q.; Runt, J.; Felder, G.; Rosenberg, G.; Snyder, A. J.; Weiss, W. J.; Lewis, J.; Werley, T. *J. Biomater. Appl.* **2000**, *14*, 349.
(23) Peebles, L. H., Jr. *Macromolecules* **1974**, *7*, 872.
(24) Ruland, W. *Colloid Polym. Sci.* **1977**, *255*, 417.
(25) Chang, S. L.; Yu, T. L.; Huang, C. C.; Chen, W. C.; Linliu, K.; Lin, T. L. *Polymer* **1998**, *39*, 3479.
(26) Lin, T.; Yu, L.; Liu, W.; Tsai, Y. *Polym. J.* **1999**, *31*, 120.
(27) Wilkes, G. L.; Abouzahr, S. *Macromolecules* **1981**, *14*, 458.
(28) Musselman, S. G.; Santosusso, T. M.; Barnes, J. D.; Sperling, L. H. *J. Polym. Sci., Polym. Phys. Ed.* **1999**, *37*, 2586.
(29) Garrett, J. T.; Siedlecki, C.; Runt, J. *Macromolecules*, submitted for publication.
(30) Baltá-Calleja, F. J.; Vonk, C. G. *X-ray Scattering of Synthetic Polymers*; Elsevier: New York, 1989.
(31) Peebles, L. H., Jr. *Macromolecules* **1976**, *9*, 58.
(32) Coleman, M. M.; Graf, J.; Painter, P. *Specific Interactions and the Miscibility of Polymer Blends*; Technomic Publishing: Lancaster, 1991.
(33) Born, L.; Crone, J.; Hespe, H.; Muller, E. H.; Wolf, K. H. *J. Polym. Sci., Polym. Phys. Ed.*, **1984**, *22*, 163.
(34) Blackwell, J.; Nagarajan, M. R.; Hoitnik, T. B. *Polymer* **1982**, *23*, 950.
(35) Quay, J. R.; Sun, R.; Blackwell, J.; Briber, R. M.; Thomas, E. L. *Polymer* **1990**, *31*, 1003.
(36) Porod, G. In *Small Angle X-ray Scattering*; Glatter, O., Kratky, O., Eds.; Academic Press: New York, 1982.
(37) Koberstein, J. T.; Morra, B.; Stein, R. S. *J. Appl. Crystallogr.* **1980**, *13*, 34.
(38) Yang, W. P.; Macosko, C. W.; Wellinghoff, S. T. *Polym. Prepr. (Am. Chem. Soc., Div. Polym. Chem.)* **1985**, *18*, 32.
(39) Seymour, R. W.; Cooper, S. L. *Macromolecules* **1973**, *6*, 48.
(40) Hesketh, T. P.; Van Bogart, J. W. C.; Cooper, S. L. *Polymer* **1981**, *22*, 1428.
(41) Hu, C. B.; Ward, R. S., Jr.; Schneider, N. S. *J. Appl. Polym. Sci.* **1982**, *27*, 2167.

MA000600I